Characterization of Inward-Rectifier K^+ Channel Inhibition by Antiarrhythmic Piperazine†

Yanping Xu and Zhe Lu*

Department of Physiology, University of Pennsylvania, 3700 Hamilton Walk, Philadelphia, Pennsylvania 19104

Received August 6, 2004; Revised Manuscript Received September 14, 2004

ABSTRACT: Strong inward-rectifier K^+ (Kir) channels play a significant role in shaping the cardiac action potential: they help produce its long plateau and accelerate its rate of repolarization. Consequently, genetic deletion of the gene encoding the strongly rectifying K^+ channel IRK1 (Kir2.1) prolongs the cardiac action potential in mice. In principle, broadening the action potential lengthens the refractory period, which may in turn be antiarrhythmogenic. Interestingly, previous studies showed that piperazine, an inexpensive and safe anthelmintic, both inhibits IRK1 channels and is antiarrhythmic in some animal preparations. This potential pharmacological benefit motivated us to further characterize the energetic, kinetic, and molecular properties of IRK1 inhibition by piperazine. We show how its blocking characteristics, in particular, its shallow voltage dependence, allow piperazine to be effective even in the presence of high-affinity polyamine blockers. We also examine the channel selectivity of piperazine and its molecular determinants.

Eighty years ago, quinidine, a diastereoisomer of the antimalarial quinine, was identified as a potent antiarrhythmic agent. Sixty years later, Onuaguluchi and Igbo (*1*) examined the anthelmintic piperazine for its potential anesthetic and antiarrhythmic effects, and compared it with lidocaine. The latter, a commonly used antiarrhythmic agent and local anesthetic, inhibits voltage-gated ion channels (*2*, *3*). Onuaguluchi and Igbo found that piperazine indeed, like lidocaine, dramatically protects toads against ouabain-induced lethal arrhythmia and prevents electrically induced arrhythmia in isolated guinea pig hearts. At antiarrhythmic concentrations, piperazine and lidocaine exhibited no negative inotropic effect. The antiarrhythmic potency of lidocaine and piperazine did not correlate with their anesthetic potency (piperazine having little effect), suggesting that the two drugs do not act on the same ion channels. In either arrhythmia model, lidocaine was 10 times more potent but 50−60 times more toxic than piperazine as measured by the LD_{50} in mice and toads. On the basis of their findings, Onuaguluchi and Igbo argued, "Piperazine citrate might therefore prove to be a much safer drug than [lidocaine] in the treatment of cardiac arrhythmia." No piperazine receptors were known in mammals until the accidental discovery that the drug inhibits a strong inward-rectifier K^+ channel, IRK1 (Kir2.1) (*4*, *5*).

Inward rectifiers (Kir)[1] make up a class of K^+ channels that can carry much larger inward K^+ currents at membrane voltages (V_m) negative to the K^+ equilibrium potential (E_K) than outward currents at voltages positive to E_K, even with equal K^+ concentrations on both sides of the membrane (*6*−*10*). Inward rectification in Kir channels arises from the strong voltage dependence of channel block by intracellular cations such as Mg^{2+} and polyamines (*11*−*15*). What initially appeared as intrinsic residual rectification in the nominal absence of known blockers turned out to be due to 1-(2-hydroxyethyl)piperazine, a contaminant of the commonly used pH buffer 4-(2-hydroxyethyl)piperazine-1-ethanesulfonic acid (HEPES) (*4*, *5*). The voltage dependence of Kir channel block results primarily from the movement of K^+ ions across the transmembrane electric field along the pore, which is energetically coupled to blocker binding and unbinding (*16*). Several sets of acidic residues (e.g., D172, E224, and E299 in IRK1), when present in the channel's inner pore, enable the channels to be inhibited by intracellular cationic blockers with rapid kinetics and high affinity (*17*−*23*). Consequently, some channels (such as IRK1) rectify strongly, while others (such as ROMK1) rectify weakly.

Forty years ago, Noble studied the role of strongly inwardly rectifying K^+ currents in the generation of cardiac action potentials (*10*, *24*). He found that inward rectification reduces K^+ conductance upon membrane depolarization and thus helps produce the long plateau in the action potential, whereas during the repolarization phase of the action potential, K^+ conductance increases again and accelerates repolarization. Recent molecular genetic studies have identified the underlying channels as IRK1 (Kir2.1) and its homologues. Deletion of the IRK1 gene in mice indeed prolongs the action potential (*25*). Slowing repolarization and broadening the action potential are expected to prolong the refractory period and may thus be antiarrhythmic (*2*). It is therefore possible that piperazine produces its antiarrhythmic effect by inhibiting Kir channels. Because of this potential clinical significance, and to understand how a relatively low-affinity blocker such as piperazine may effectively slow repolarization even in the presence of high-affinity endogenous blockers, we systematically investigated the biophysi-

† This study was supported by NIH Grant GM61929.

* To whom correspondence should be addressed: Department of Physiology, University of Pennsylvania, D302A Richard Building, 3700 Hamilton Walk, Philadelphia, PA 19104. Telephone: (215) 573-7711. Fax: (215) 573-1940. E-mail: zhelu@mail.med.upenn.edu.

[1] Abbreviations: Kir, inward-rectifier K^+ channel; HEPES, 4-(2-hydroxyethyl)piperazine-1-ethanesulfonic acid.

10.1021/bi0483099 CCC: $27.50
Published on Web 11/19/2004

cal and molecular properties of inhibition of IRK1 by piperazine.

METHODS

Molecular Biology and Oocyte Preparation. The cDNAs of IRK1 and Shaker with inactivation removed (*26*−*28*) were subcloned in the pGEM-HESS plasmid (*29*), that of ROMK1 (*30*) in the pSPUTK plasmid (for simplicity, we will refer to Shaker with inactivation removed as Shaker). All mutant cDNAs were obtained through PCR-based mutagenesis and confirmed by DNA sequencing. The cRNAs were synthesized with T7 polymerase (Promega Corp., Madison, WI) using linearized cDNAs as templates. Oocytes harvested from *Xenopus laevis* (Xenopus One, Ann Arbor, MI) were incubated in a solution containing 82.5 mM NaCl, 2.5 mM KCl, 1.0 mM $MgCl_2$, 5.0 mM HEPES (pH 7.6), and 2−4 mg/mL collagenase. The oocyte preparation was agitated at 80 rpm for 60−90 min. It was then rinsed thoroughly and stored in a solution containing 96 mM NaCl, 2.5 mM KCl, 1.8 mM $CaCl_2$, 1.0 mM $MgCl_2$, 5 mM HEPES (pH 7.6), and 50 μg/mL gentamycin. Defolliculated oocytes were selected and injected with RNA at least 2 and 16 h, respectively, after collagenase treatment. All oocytes were stored at 18 °C.

Recordings and Solutions. Macroscopic currents were recorded from inside-out membrane patches of *Xenopus* oocytes heterologously expressing IRK1, ROMK1, or Shaker channels using an Axopatch 200B amplifier (Axon Instruments, Inc., Foster City, CA), filtered at 5 kHz and sampled at 25 kHz. Unless specified otherwise, to elicit Kir currents the voltage across the membrane patch was first hyperpolarized from the 0 mV holding potential to −100 mV and then stepped to various test voltages between −100 and 100 mV and back to 0 mV. Background leak current correction was as previously described (*4*, *18*). Solutions on both sides of the patch contained 5 mM K_2EDTA, 10 mM "K_2HPO_4 + KH_2PO_4" in a ratio yielding a pH of 7.6, and sufficient KCl to bring the total K^+ concentration to 100 mM (*4*, *5*). The low-K^+ extracellular solution contained 4 mM KCl, 1 mM $MgCl_2$, 0.3 mM $CaCl_2$ (no EDTA), 10 mM Na_2HPO_4 + NaH_2PO_4 in a ratio yielding a pH of 7.6, and sufficient NaCl to bring the total Na^+ concentration to 96 mM. To elicit Shaker currents, the voltage across the membrane patch was depolarized from the −100 mV holding potential to various test voltages between −100 and 100 mV and then back to −100 mV. The recording solutions contained 100 mM K^+ as described above, except that the extracellular solution contained 0.3 mM Ca^{2+} and 1.0 mM Mg^{2+} but no EDTA. The piperazine-containing intracellular solutions had the same final pH. All chemicals were purchased from Fluka Chemical Corp.

RESULTS

To compare IRK1 channel block by piperazine with that by physiological blockers such as spermine, we examined its characteristics both in the commonly employed symmetric 100 mM K^+ solutions and in the 4 mM K^+ extracellular solution. Detailed comparison of the fundamental blocking characteristics of the two blockers reveals how piperazine can still affect IRK1 currents in the presence of the high-affinity endogenous blocker spermine. We carried out the study with mouse IRK1 because that clone was used in nearly all previous biophysical studies. Mouse IRK1 and human IRK1 differ at only five residues, none of them in the ion conduction pore.

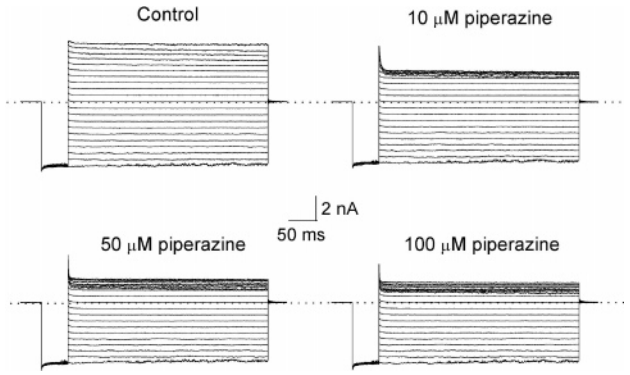

FIGURE 1: Inhibition of IRK1 channels by intracellular piperazine. Shown are currents of IRK1 channels, recorded in the absence (control) or presence of piperazine at the indicated concentrations, and with the voltage protocol described in Methods. Dotted lines define zero current levels.

Inhibition of IRK1 Channels by Piperazine. Figure 1 shows IRK1 currents recorded in the absence or presence of intracellular piperazine at three representative concentrations. In the absence of piperazine, the absolute magnitude of inward and outward currents at corresponding negative and positive voltages is comparable; i.e., the $I-V$ relation is approximately linear (Figure 2A). Dose-dependent outward current block by piperazine is enhanced by membrane depolarization (Figure 1). The voltage-dependent channel inhibition renders the $I-V$ curves inwardly rectifying (Figure 2A). The fraction of current not inhibited at three representative membrane voltages is plotted against the concentration of piperazine in Figure 2B. The curves through the data are fits of an equation describing a model in which one piperazine molecule blocks one channel. The K_d values obtained from the fits are plotted against the membrane voltage in Figure 2C. The line fitted to the data is a Boltzmann function, yielding a K_d(0 mV) of 1.17 ± 0.05 mM (mean ± standard error of the mean) and an apparent valence (Z) of 1.19 ± 0.02.

In the presence of 10−100 μM piperazine, the kinetics of channel inhibition at positive voltages are sufficiently slow for quantitative analysis. For illustration, we show in Figure 3A the current transients elicited by voltage pulses from the 0 mV holding potential to 70 mV. The curves superimposed on the current traces are single-exponential fits. The reciprocal of the time constants ($1/\tau$) obtained from such fits is plotted against the piperazine concentration for three representative voltages (Figure 3B). We fitted the concentration dependence of $1/\tau$ with straight lines to obtain the slope which reflects k_{on}, the apparent (second-order) rate constant of channel inhibition by piperazine. To examine the voltage dependence of k_{on}, we plotted it against membrane voltage (Figure 3C). The linear fit to the data in Figure 3C is a Boltzmann function, which yields a k_{on}(0 mV) of 5.56 (±0.46) × 10^6 M^{-1} s^{-1} and a z_{on} of 0.20 ± 0.03. As in the case of channel block by alkylamines, the voltage dependence of k_{on} is shallow, consistent with the channel becoming blocked as soon as the blocker encounters the innermost K^+ ion in the pore (*31*, *32*). In the case that piperazine block of

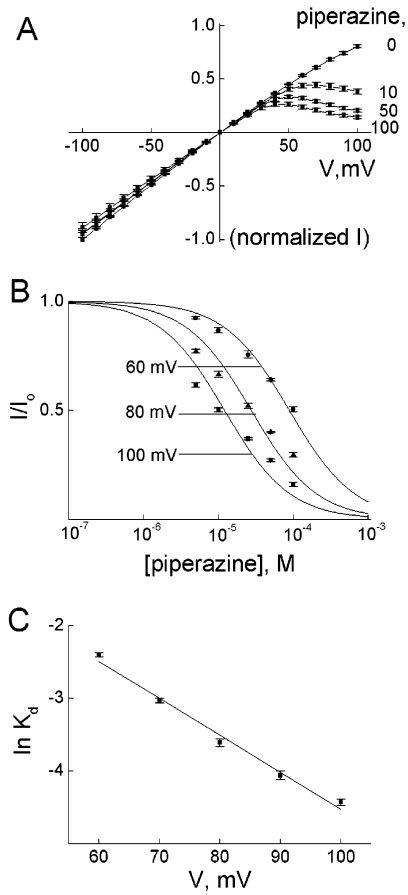

FIGURE 2: Voltage dependence of IRK1 channel inhibition by piperazine. (A) Averaged steady-state $I-V$ curves in the absence and presence of piperazine at the indicated concentrations. (B) The fraction of current not blocked [mean ± the standard error of the mean (sem); $n = 5$] is plotted against piperazine concentration for three representative voltages. The curves through the data are fits of the hyperbolic inhibition equation $I/I_o = K_d/(K_d + [\text{piperazine}])$. (C) The natural logarithm of the resulting K_d values (mean ± sem; $n = 5$) is plotted against membrane voltage. The line through the data is a fit of the Boltzmann function, yielding a $K_d(0\ \text{mV})$ of 1.17 ± 0.05 mM and an apparent valence (Z) of 1.19 ± 0.02.

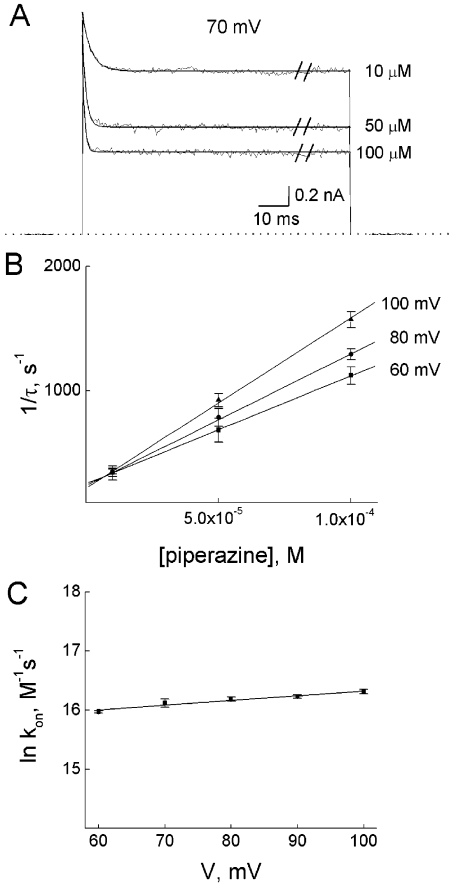

FIGURE 3: Relaxation kinetics of voltage jump-induced IRK1 currents in the presence of piperazine. (A) Currents elicited by stepping the membrane voltage from 0 to 70 mV at three piperazine concentrations. The curves superimposed on the data are single-exponential fits. The dotted line defines the zero current level. (B) Reciprocals of the time constants of current transients (mean ± sem; $n = 5$) obtained from fits such as those shown in panel A are plotted against the piperazine concentration for three representative voltages. The lines through the data are linear fits. (C) The natural logarithm of the rate constant for formation of the blocked state (k_{on}, determined from the slopes in panel B) is plotted against membrane voltage. The line through the data is a fit of the Boltzmann function, yielding a $k_{on}(0\ \text{mV})$ of 5.56 (± 0.46) × 10^6 M^{-1} s^{-1} (mean ± sem; $n = 5$) and a z_{on} of 0.20 ± 0.03.

IRK1 is truly a simple bimolecular reaction $k_{off}(0\ \text{mV}) = K_d k_{on} = 6.50 \times 10^3\ \text{s}^{-1}$ and $z_{off} = Z - z_{on} = 0.99$.

Channel Selectivity of Piperazine. To determine whether the observed piperazine inhibition is specific, we examined its effect on the well-characterized ROMK1 inward-rectifier (Kir1.1) and Shaker voltage-gated K^+ channels. Figure 4 shows the currents of ROMK1 and Shaker channels in the absence or presence of 0.1 and 1 mM intracellular piperazine. Although 0.1 mM piperazine causes profound inhibition of the IRK1 current (Figure 1), at this or even higher concentrations it had a negligible effect on either ROMK1 or Shaker currents. Thus, the observed inhibitory effect of piperazine on IRK1 is relatively specific.

Effects of Mutations in IRK1 on Channel Inhibition by Piperazine. We examined the effects on channel affinity for piperazine of neutralizing residue D172 in M2, and E224/E299 in the C-terminus, where mutations affect IRK1 inhibition by many intracellular cationic blockers (*17*−*23*). Residue D172 in M2 lines the part of the ion conduction pore that is internal to the ion selectivity filter formed by the signature sequence (*33*−*35*). Figure 5 shows currents through D172N mutant IRK1 channels, recorded in the absence or presence of three representative piperazine concentrations. Piperazine inhibits wild-type and D172N mutant channels in a comparable manner. The $I-V$ curves of the D172N channels in the absence or presence of various concentrations of piperazine are plotted in Figure 6A. Like that of wild-type channels, the $I-V$ curve of D172N mutant channels is approximately linear in the absence of piperazine. The strongly voltage-dependent inhibition of the mutant channels by piperazine renders the $I-V$ curve inwardly rectifying. To examine the K_d quantitatively, we plotted, in Figure 6B, the fraction of current not inhibited against the piperazine concentration and fitted the relation with an equation for 1:1 stoichiometry between the channel and blocker. The K_d values obtained from these fits are then plotted against membrane voltage in Figure 6C. The line fitted to the data in Figure 6C is a Boltzmann function, for which $K_d(0\ \text{mV}) = 2.98 \pm 0.16$ mM and $Z = 1.25 \pm 0.13$. Thus, the D172N mutation reduces the channel's affinity for piperazine ~2.5-fold, with little effect on the apparent valence.

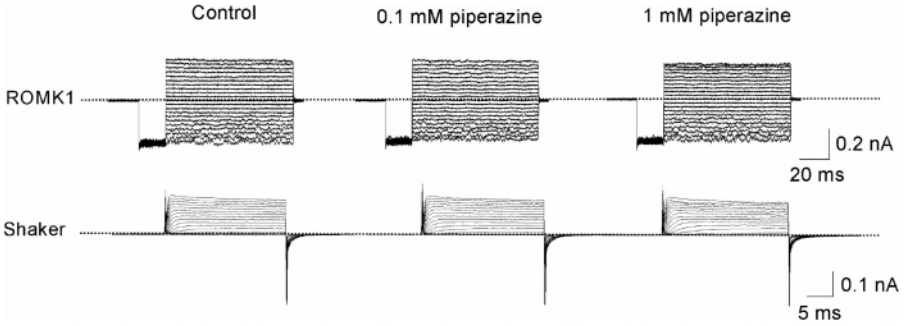

FIGURE 4: Effects of intracellular piperazine on ROMK1 and Shaker channels. Shown are ROMK1 and Shaker currents recorded in the absence (control) or presence of 0.1 or 1.0 mM piperazine, and with the voltage protocols described in Methods. Dotted lines define zero current levels.

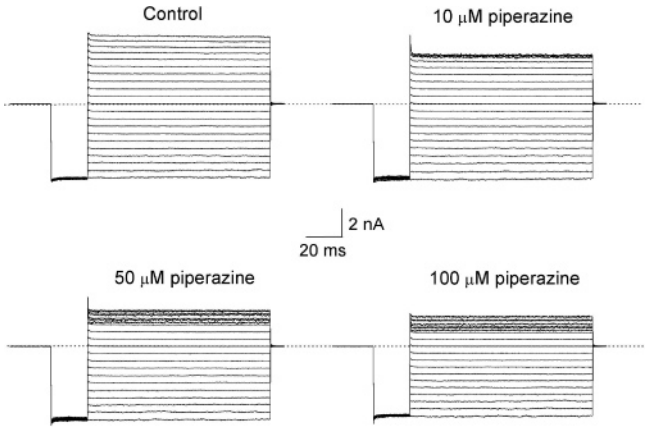

FIGURE 5: Inhibition of D172N mutant IRK1 channels by intracellular piperazine. Shown are currents through the D172N channels, recorded in the absence (control) or presence of piperazine at the indicated concentrations. Dotted lines define zero current levels.

We next neutralized C-terminal residues E224 and E299 that form a ring at the more internal part of the pore (*35*, *36*). Figure 7 shows currents through the double-mutant channels, recorded in the absence or presence of 0.1 or 1.0 mM piperazine. As shown previously, these double-mutant channels carry larger inward currents at negative voltages than outward currents at the corresponding positive voltages, even in the absence of blockers (*22*, *31*). Unlike wild-type or D172N mutant channels, the double-mutant channels are barely affected by piperazine at concentrations as high as 1 mM. Thus, residues E224 and E299 seem to be critical for the channel inhibition by piperazine.

Effect of Extracellular K^+ on the Affinity of IRK1 for Piperazine. Panels A and B of Figure 8 show wild-type IRK1 currents recorded in the absence or presence of 0.1 mM piperazine. The intracellular solution contained 100 mM K^+, whereas the extracellular solution contained 4 mM K^+, predicting a reversal potential of approximately −80 mV. However, the observed reversal potential was approximately −70 mV, indicating that the effective extracellular K^+ concentration was ∼7 mM, which was most probably due to an increased K^+ concentration near the extracellular side of the membrane patch caused by the K^+ efflux, a phenomenon commonly termed extracellular K^+ accumulation. In Figure 8C, we plot the K_d, determined as shown in Figure 2, against membrane voltage. Extrapolation of the Boltzmann fit yields a K_d(0 mV) of 0.41 mM. Thus, reducing the extracellular K^+ concentration from 100 mM to a nominal value of 4 mM increases the affinity of the channel for piperazine ∼3-fold.

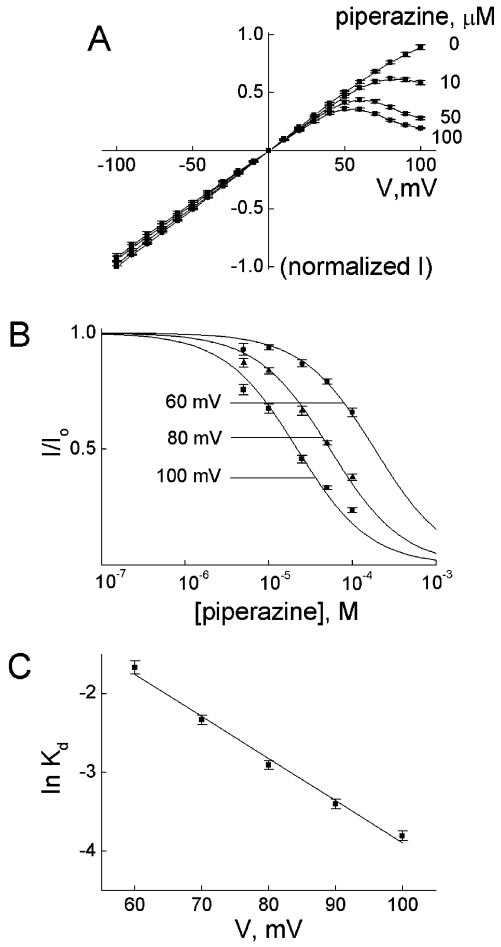

FIGURE 6: Voltage dependence of piperazine inhibition of the D172N mutant IRK1 channels. (A) Averaged steady-state $I-V$ curves in the absence and presence of piperazine at the indicated concentrations. (B) The fraction of current not blocked (mean ± sem; $n = 7$) is plotted against piperazine concentration for three representative voltages. The curves through the data are fits to the hyperbolic equation $I/I_o = K_d/(K_d + [\text{piperazine}])$. (C) The natural logarithm of the K_d values (mean ± sem; $n = 7$) obtained from the fits in panel B is plotted against membrane voltage. The line through the data is a fit of the Boltzmann function, yielding a K_d(0 mV) of 2.98 ± 0.16 mM and a Z of 1.25 ± 0.13.

DISCUSSION

Outward IRK1 currents are significantly inhibited by trace amounts of contaminating hydroxyethylpiperazine in com-

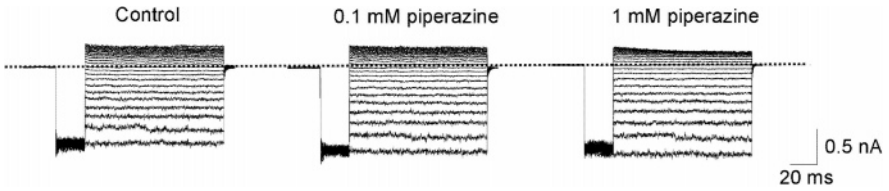

FIGURE 7: Effect of piperazine on IRK1 channels containing a double mutation. Shown are currents through E224G/E299S mutant channels, recorded in the absence (control) or presence of piperazine at the indicated concentrations. The dotted line defines the zero current level.

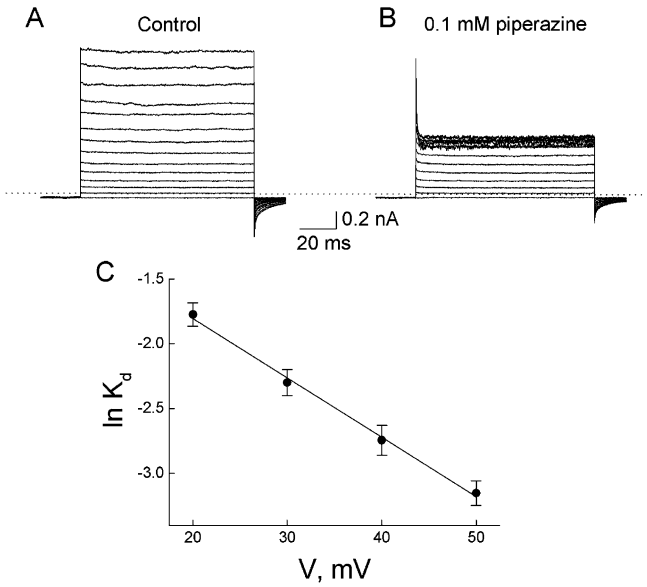

FIGURE 8: Effect of extracellular K^+ concentration on IRK1 inhibition by intracellular piperazine. Shown are currents through IRK1 channels in the absence (control, A) or presence (B) of 0.1 mM piperazine. The dotted line defines the zero current level. Nominal K^+ concentrations in the extracellular and intracellular solutions are 4 and 100 mM, respectively. During the recording, the membrane voltage was stepped from the −80 mV holding potential to various voltages between −80 and 50 mV in 10 mV increments, and then back to the holding potential. (C) The natural logarithm of K_d values (mean ± sem; $n = 3$), determined as shown in Figure 2, is plotted against membrane voltage. The line through the data is a fit of the Boltzmann function, yielding a K_d(0 mV) of 0.41 ± 0.03 mM and an apparent valence (Z) of 1.17 ± 0.05.

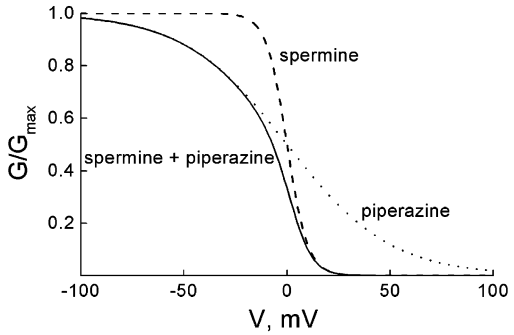

FIGURE 9: Simulated $G-V$ curves. The curves are drawn by assuming that the $G-V$ relation of the channels in the presence of either spermine (- - -) or piperazine (• • •) follows the Boltzmann function, where valences are 5 and 1 for spermine and piperazine, respectively, and the concentration of each blocker is set equal to the corresponding K_d(0 mV). The solid curve represents the case in which both spermine and piperazine are present.

mercially available HEPES, a common pH buffer in artificial intracellular solutions (*4*, *5*). Both hydroxyethylpiperazine and piperazine itself inhibit the IRK1 channels in a comparably voltage-dependent manner (Figures 1 and 2; *5*). There is no evidence to date that HEPES significantly inhibits any other type of K^+ channel in usual experimental voltage ranges, which is consistent with our observation that piperazine blocks the strong-rectifier IRK1 and not weak-rectifier ROMK1 or voltage-gated Shaker K^+ channels.

The observed selective inhibition of IRK1 (and possibly of other strong rectifiers, including GIRK channels) by piperazine may be therapeutically beneficial and is mechanistically interpretable. The selective affinity of piperazine for strong rectifiers is not surprising, because the presence of several specific sets of acidic residues in these channels makes them be blocked by intracellular cationic blockers with rapid kinetics and high affinity (*17*−*23*). In fact, neutralizing both E224 and E299 in the inner pore renders IRK1 channels nearly insensitive to piperazine at concentrations as high as 1 mM (Figure 7).

On the basis of the electrophysiological studies of Noble (*10*, *24*) and the genetic knockout experiments of Zaritzsky et al. (*25*), inhibition of IRK1 is expected to prolong the cardiac action potential and therefore the refractory period, i.e., to be potentially antiarrhythmic. In light of this, the apparent selective inhibition of IRK1 (and possibly of other strong rectifiers, including GIRK channels) may underlie the antiarrhythmic effects of piperazine reported by Onuaguluchi and Igbo 20 years ago (*1*).

One may ask how the relatively low-affinity piperazine can still affect the IRK1 current even though all IRK1 channels in native cardiac cells are already blocked by endogenous high-affinity blockers, such as spermine, at sufficiently depolarized potentials. The answer resides in the very different voltage dependence of channel block by spermine and by piperazine. To illustrate this, we show (Figure 9) idealized $G-V$ relations in the presence of spermine or piperazine, which (for simplicity) are described in both cases by a Boltzmann function in which the blocker concentration is set equal to the corresponding K_d(0 mV). However, apparent valence is typically much higher for spermine ($Z = 5$ (*5*, *32*)) than for piperazine ($Z = 1$). Since block by spermine (dashed curve) is steeply voltage-dependent, the channels become unblocked within a very narrow voltage range upon hyperpolarization, and the resulting K^+ current, as Noble (*10*, *24*) concluded, accelerates the repolarizing phase of the action potential. On the other hand, channel block by piperazine (dotted curve) is much less voltage-dependent so that channel unblock in the presence of piperazine occurs over a much wider voltage range even when both spermine and piperazine are present (solid curve). Consequently, in the latter case, during the repolarizing phase of the action potential, outward K^+ current through IRK1 channels would be diminished at each voltage, resulting in a broadened action potential.

Such a scenario requires not only that spermine block be more voltage-dependent than piperazine block but also that

a significant part of piperazine's $G-V$ curve occur in a voltage range more negative than spermine's. For a given blocker, the midpoint voltage on the $G-V$ curve is determined by [blocker]/K_d(0 mV). Although the concentration of spermine in various types of cardiac myocyte is unknown, it is undoubtedly much higher than the blocker's K_d(0 mV), resulting in a leftward shift of the $G-V$ curve. This would place spermine's midpoint voltage in the negative region, yet within the limits imposed by the observed outward conductance over the physiological negative voltage range. Piperazine's midpoint voltage is, of course, determined by the drug's dose.

Furthermore, under physiological conditions, Kir channels are most likely blocked not only by spermine but also by Mg^{2+} and other polyamines with different apparent affinities and voltage dependencies. Despite this, near the reversal potential, the channels are not fully blocked and carry significant outward currents, which are critical for their function and can in principle be further reduced even by a blocker, such as piperazine, which exhibits a relatively low affinity and a weak voltage dependence.

Piperazine [p$K_a \sim 4$ (*37*)] citrate, the medicinal form available in the United States, is an inexpensive vermicide used in both adults and children at 75 mg/kg, up to a maximum of 3.5 g per single daily dose, and is rapidly absorbed after oral administration (*2*). Piperazine has a high therapeutic index and has been used without ill effect during pregnancy.

The shape and duration of action potentials in individual myocytes throughout the myocardium are notoriously heterogeneous. Prolonging the cardiac action potential, and thus the $Q-T$ interval in the electrocardiogram, can be antiarrhythmic, arrhythmogenic, or inconsequential. For example, although a prolonged $Q-T$ interval due to deletion of the IRK1 gene in mice causes no significant arrhythmia (*25*), patients with Andersen's syndrome due to an IRK1 mutation exhibit prolonged $Q-T$ intervals and various forms of arrhythmia (*38*). Some Kv channel blockers are antiarrhythmic, whereas others are arrhythmogenic (*2*). Since repolarization of the cardiac action potential is mainly due to outward K^+ currents through Kv, including HERG channels, modest inhibition of IRK1 channels, unlike reduced HERG channel activity (*39*), may not delay repolarization sufficiently to cause lethal long-$Q-T$ conditions. Thus, it is not surprising that no significant cardiac side effects of piperazine have been reported in otherwise normal individuals.

Together, its selectivity and documented safety make piperazine (or a derivative) a candidate drug for treating arrhythmia. We hope our molecular and biophysical characterization of IRK1 block will stimulate interest in further research on the electrophysiological effects of piperazine in isolated cardiac preparations and in whole animals.

ACKNOWLEDGMENT

We thank P. De Weer for critical review of our manuscript, K. Ho and S. Hebert for ROMK1 cDNA, L. Y. Jan for IRK1 cDNA, and J. Yang for IRK1 cDNA subcloned in the pGEM-HESS vector.

REFERENCES

1. Onuaguluchi, G., and Igbo, I. N. A. (1985) Comparative antiarrhythmic and local anaesthetic effects of piperazine citrate and lignocaine hydrochloride, *Arch. Int. Pharmacodyn. Ther. 274*, 253−266.
2. Hardman, J. G., Limbird, L. E., Molinoff, P. B., Ruddon, R. W., and Gilman, A. G., Eds. (1996) *Goodman & Gilman's The Pharmacological Basis of Therapeutics*, 9th ed., McGraw-Hill, New York.
3. Hille, B. (2001) *Ion channels of excitable membranes*, 3rd ed., Sinauer Associates, Sunderland, MA.
4. Guo, D., and Lu, Z. (2000) Pore block versus intrinsic gating in the mechanism of inward rectification in the strongly-rectifying IRK1 channel, *J. Gen. Physiol. 116*, 561−568.
5. Guo, D., and Lu, Z. (2002) IRK1 inward rectifier K^+ channels exhibit no intrinsic rectification, *J. Gen. Physiol. 120*, 539−551.
6. Katz, B. (1949) Les constantes électriques de la membrane du muscle, *Arch. Sci. Physiol. 3*, 285−299.
7. Hodgkin, A. L., and Horowicz, P. (1959) The influence of potassium and chloride ions on the membrane potential of single muscle fibres, *J. Physiol. 148*, 127−160.
8. Hagiwara, S., and Takahashi, K. (1974) The anomalous rectification and cation selectivity of the membrane of a starfish egg cell, *J. Membr. Biol. 18*, 61−80.
9. Hagiwara, S., Miyazaki, S., and Rosenthal, N. P. (1976) Potassium current and the effect of cesium on this current during anomalous rectification of the egg cell membrane of a starfish, *J. Gen. Physiol. 67*, 621−638.
10. Noble, D. (1965) Electrical properties of cardiac muscle attributable to inward going (anomalous) rectification, *J. Cell. Compar. Physiol. 66*, 127−136.
11. Matsuda, H., Saigusa, A., and Irisawa, H. (1987) Ohmic conductance through the inwardly rectifying K^+ channel and blocking by internal Mg^{2+}, *Nature 325*, 156−159.
12. Vandenberg, C. A. (1987) Inward rectification of a potassium channel in cardiac ventricular cells depends on internal magnesium ions, *Proc. Natl. Acad. Sci. U.S.A. 84*, 2560−2564.
13. Lopatin, A. N., Makhina, E. N., and Nichols, C. G. (1994) Potassium channel block by cytoplasmic polyamines as the mechanism of intrinsic rectification, *Nature 372*, 366−369.
14. Ficker, E., Taglialatela, M., Wible, B. A., Henley, C. M., and Brown, A. M. (1994) Spermine and spermidine as gating molecules for inward rectifier K^+ channels, *Science 266*, 1068−1072.
15. Fakler, B., Brandle, U., Glowatzki, E., Weidemann, S., Zenner, H. P., and Ruppersberg, J. P. (1995) Strong voltage-dependent inward rectification of inward rectifier K^+ channels is caused by intracellular spermine, *Cell 80*, 149−154.
16. Lu, Z. (2004) Mechanism of rectification in inward-rectifier K^+ channels, *Annu. Rev. Physiol. 66*, 103−129.
17. Stanfield, P. R., Davies, N. W., Shelton, P. A., Sutcliffe, M. J., Khan, I. A., Brammar, W. J., Standen, N. B., and Conley, E. C. (1994) A single aspartate residue is involved in both intrinsic gating and blockage by Mg^{2+} of the inward rectifier, IRK1, *J. Physiol. 478*, 1−6.
18. Lu, Z., and MacKinnon, R. (1994) Electrostatic tuning of Mg^{2+} affinity in an inward-rectifier K^+ channel, *Nature 371*, 243−246.
19. Wible, B. A., Taglialatela, M., Ficker, E., and Brown, A. M. (1994) Gating of inwardly rectifying K^+ channels localized to a single negatively charged residue, *Nature 371*, 246−249.
20. Yang, J., Jan, Y. N., and Jan, L. Y. (1995) Control of rectification and permeation by residues in two distinct domains in an inward rectifier K^+ channel, *Neuron 14*, 1047−1054.
21. Taglialatela, M., Ficker, E., Wible, B. A., and Brown, A. M. (1995) C-Terminus determinants for Mg^{2+} and polyamine block of the inward rectifier K^+ channel IRK1, *EMBO J. 14*, 5532−5541.
22. Kubo, Y., and Murata, Y. (2001) Control of rectification and permeation by two distinct sites after the second transmembrane region in Kir2.1 K^+ channel, *J. Physiol. 531*, 645−660.
23. Taglialatela, M., Wible, B. A., Caporaso, R., and Brown, A. M. (1994) Specification of pore properties by the carboxyl terminus of inwardly rectifying K^+ channels, *Science 264*, 844−847.
24. Noble, D. (1962) A modification of Hodgkin-Huxley equations applicable to Purkinje fibre action and pace-maker potentials, *J. Physiol. 160*, 317−352.
25. Zaritsky, J. J., Redell, J. B., Tempel, B. L., and Schwarz, T. L. (2001) The consequence of disrupting cardiac inwardly rectifying K^+ current (*I*K1) as revealed by the targeted deletion of the murine *Kir2.1* and *Kir2.2* genes, *J. Physiol. 533*, 697−710.
26. Kubo, Y., Baldwin, T. J., Jan, Y. N., and Jan, L. Y. (1993) Primary structure and functional expression of a mouse inward rectifier potassium channel, *Nature 362*, 127−133.

27. Hoshi, T., Zagotta, W. N., and Aldrich, R. W. (1990) Biophysical and molecular mechanisms of *Shaker* potassium channel inactivation, *Science 250*, 533−538.
28. Zagotta, W. N., Hoshi, T., and Aldrich, R. W. (1990) Restoration of inactivation in mutants of Shaker potassium channels by a peptide derived from ShB, *Science 250*, 568−571.
29. Liman, E. R., Tytgat, J., and Hess, P. (1992) Subunit stoichiometry of a mammalian K^+ channel determined by construction of multimeric cDNAs, *Neuron 9*, 861−871.
30. Ho, K., Nichols, C. G., Lederer, W. J., Lytton, J., Vassilev, P. M., Kanazirska, M. V., and Hebert, S. C. (1993) Cloning and expression of an inwardly rectifying ATP-regulated potassium channel, *Nature 362*, 31−38.
31. Guo, D., Ramu, Y., Klem, A. M., and Lu, Z. (2003) Mechanism of rectification in inward-rectifier K^+ channels, *J. Gen. Physiol. 121*, 261−275.
32. Guo, D., and Lu, Z. (2003) Interaction mechanisms between polyamines and IRK1 inward rectifier K^+ channels, *J. Gen. Physiol. 122*, 485−500.
33. Doyle, D. A., Morais, C. J., Pfuetzner, R. A., Kuo, A., Gulbis, J. M., Cohen, S. L., Chait, B. T., and MacKinnon, R. (1998) The structure of the potassium channel: molecular basis of K^+ conduction and selectivity, *Science 280*, 69−77.
34. Zhou, M., Morais-Cabral, J. H., Mann, S., and MacKinnon, R. (2001) Potassium channel receptor site for the inactivation gate and quaternary amine inhibitors, *Nature 411*, 657−661.
35. Kuo, A., Gulbis, J. M., Antcliff, J. F., Rahman, T., Lowe, E. D., Zimmer, J., Cuthbertson, J., Ashcroft, F. M., Ezaki, T., and Doyle, D. A. (2003) Crystal structure of the potassium channel KirBac1.1 in the closed state, *Science 300*, 1922−1926.
36. Nishida, M., and MacKinnon, R. (2002) Structural basis of inward rectification: Cytoplasmic pore of the G protein-gated inward rectifier GIRK1 at 1.8 Å resolution, *Cell 111*, 957−965.
37. Budavari, S., Ed. (1996) *The Merck Index*, 12th ed., Merck Research Laboratories, Whitehouse Station, NJ.
38. Plaster, N. M., Tawil, R., Tristani-Firouzi, M., Canun, S., Bendahhou, S., Tsunoda, A., Donaldson, M. R., Iannaccone, S. T., Brunt, E., Barohn, R., Clark, J., Deymeer, F., George, A. L., Jr., Fish, F. A., Hahn, A., Nitu, A., Ozdemir, C., Serdaroglu, P., Subramony, S. H., Wolfe, G., Fu, Y. H., and Ptacek, L. J. (2001) Mutations in Kir2.1 cause the developmental and episodic electrical phenotypes of Andersen's syndrome, *Cell 38*, 511−519.
39. Curran, M. E., Splawski, I., Timothy, K. W., Vincent, G. M., Green, E. D., and Keating, M. T. (1995) A molecular basis for cardiac arrhythmia: HERG mutations cause long QT syndrome, *Cell 80*, 795−803.

BI0483099